Electronic Supplementary Material (ESI) for RSC Advances.

Supporting Information

In vivo

Curcumin-Polydopamine Nanoparticles Alleviate Ferroptosis by Iron Chelation and Inhibition of Oxidative Stress Damage

Li Lei,[a, b] Jiali Yuan,[b] Qingqing Yang,[c] Qiuxia Tu,[b] Haijun Yu,[d] Liangzhao Chu,*[a] Lei Tang,*[c] and Chunlin Zhang*[b]

a. Department of Neurosurgery, the Affiliated Hospital of Guizhou Medical University, Guiyang, Guizhou, China.

b. Engineering Research Center for Molecular Medicine, School of Basic Medical Science, Guizhou Medical University, Guiyang 550025, China.

c. Guizhou Provincial Engineering Technology Research Center for Chemical Drug R&D, College of Pharmacy, Guizhou Medical University, Guiyang, 550025, China.

d. Center of Pharmaceutics, Shanghai Institute of Materia Medica, Chinese Academy of Sciences, Shanghai 201203, China.

Table of Contents

1. Experimental procedures

1.1 Cell culture.

PC12 cells were cultivated in high-glucose Dulbecco's modified Eagle medium, supplemented with 1% glutamine, 10% fetal bovine serum, and 1% penicillin-streptomycin. This culture was stored at 37°C in a 5% CO_2 incubator, and the medium was renewed every 24 h. Upon attaining 80%–90% confluence, we subjected the cells to trypsin digestion (0.25%). Subsequent experiments were conducted with cells in the logarithmic growth phase.

1.2 Nematode and culture conditions.

The nematode *C. elegans* wild-type Bristol (N2) strains、transgenic NL590 1 strain [*unc-54p::α-synuclein::YFP+unc-119(+)*]、BZ555 strain [*Pdat-1::GFP*]、DA 2123 strain [*lgg-1p::GFP::lgg-1+rol-6(su1006)*]、PD4251 [*myo-3p::mitochondrial GFP*]were acquired from the Caenorhabditis Genetics Center (University of Minnesota, Saint Paul, MN, USA). All nematodes were cultured on nematode growth medium (NGM) agar plates seeded with the uracil auxotroph Escherichia coli OP50 (serving as a food source) at 20 ℃.

2. Supplementary Figures

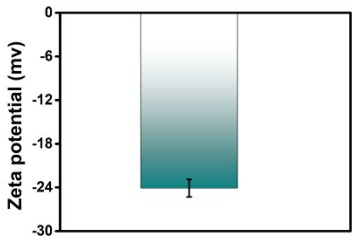

Fig. S1 Zeta potential of Cur-PDA.

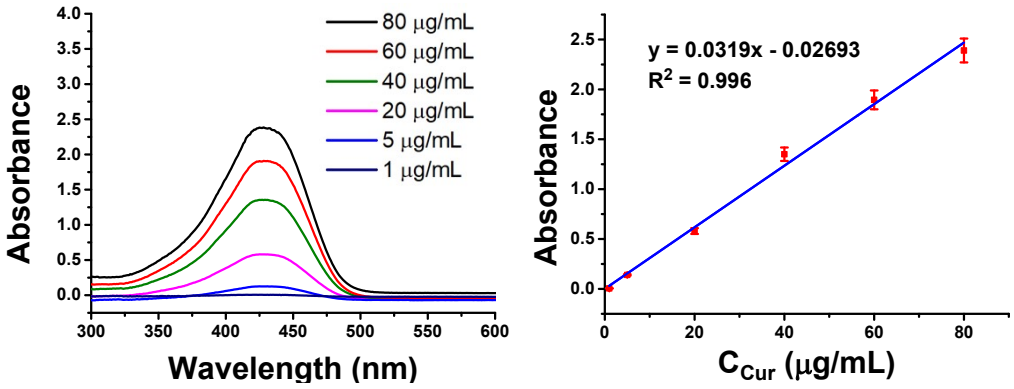

Fig. S2 Ultraviolet-visible absorption spectra of Cur at different concentrations, and calibration curve of the adsorption peak at 435 nm for different Cur concentrations (1–80 μg/mL). The data are provided as mean values with corresponding s.d. (n = 3).

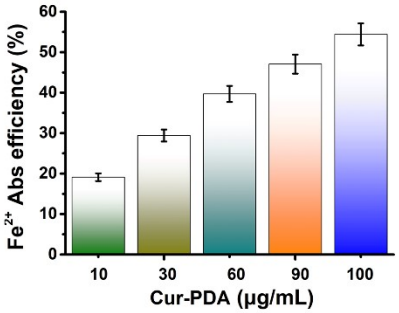

Fig. S3 Chelation efficiency of Cur-PDA for Fe^{2+}.

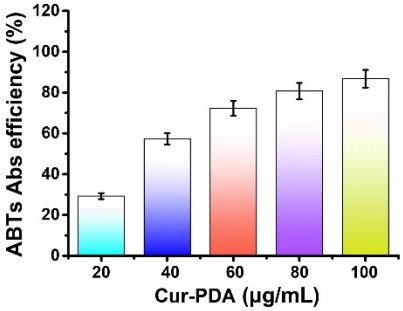

Fig. S4 Scavenging efficiency of Cur-PDA on ABTS free radicals.

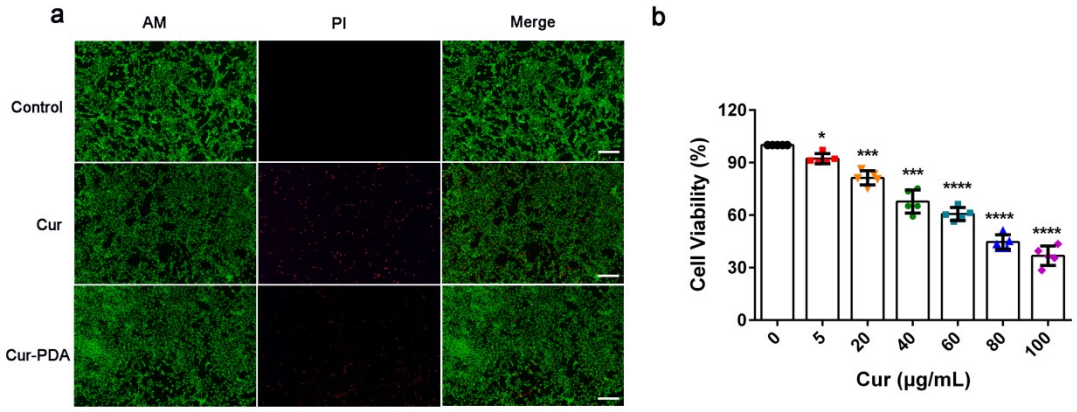

Fig. S5 (a) AM/PI staining of PC12 cells following 24 h of treatment with Cur (5 μg/mL) and Cur-PDA (10 μg/mL). (b) Cell survival rate of PC12 cells following 24 h of treatment with varying Cur concentrations.

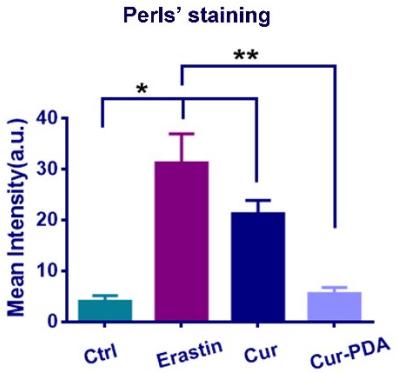

Fig. S6 Quantitative the blue blots in the graph of Fig. 4 (c).

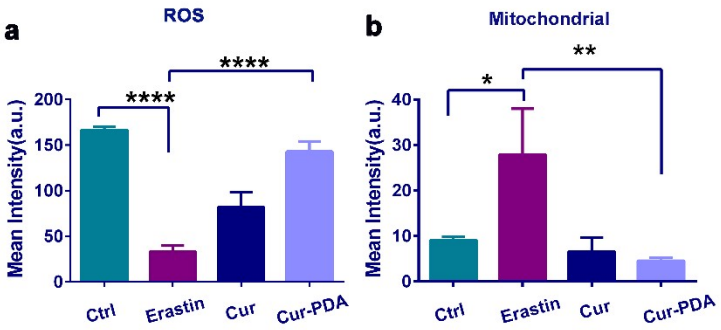

Fig. S7 (a) Quantitative analysis of ROS fluorescence from Fig. 5(a). (b) Quantitative mitochondrial fluorescence graph from Fig. 5(b).